Upper bound for the thermal emission of a hot nanoemitter assisted by a cold nanoantenna

Emilie Sakat, Léo Wojszvzyk, Jean-Jacques Greffet, Jean-Paul Hugonin, Christophe Sauvan

Upper bound for the thermal emission of a hot nanoemitter assisted by a cold nanoantenna

Sakat E.[a,b], Wojszvzyk L.[a], Greffet J.-J.[a], Hugonin J.-P.[a], and Sauvan C.[a]

[a]Universite Paris-Saclay, Institut d'Optique Graduate School, CNRS, Laboratoire Charles Fabry, 91127, Palaiseau, France
[b]Universite Paris Saclay, Center for Nanoscience and Nanotechnology, C2N UMR 9001, CNRS, 91120 Palaiseau, France

ABSTRACT

In the last decades, designs of most incandescent sources have been realized by heating the whole device. Here we propose a novel approach consisting in taking advantage of hot nanoemitters that can be cooled in a few tens of nanoseconds. It offers a new opportunity for high speed modulation and for enhanced agility in the active control of polarization, direction and wavelength of emission. To compensate the weak thermal emission of isolated nanoemitters, we propose to insert them in some complex environments, such as e.g. the gap of cold nanoantenna, which allow a significant thermal emission enhancement of the hot nanovolume. In order to optimize this kind of device, a fully vectorial upper bound for the thermal emission of a hot nanoparticle in a cold environment is derived. This criterion is very general since it is equivalent to an absorption cross-section upper bound for the nanoparticle. Moreover, it is an intrinsic characteristic of the environment regardless of the nanoparticle, so it allows to decouple the design of the environment from the one of the hot nanovolume. It thus provides a good figure of merit to compare the ability of different systems to enhance thermal emission of hot nanoemitters.

Keywords: Nanophotonics, Active and tunable device, Infrared, Nanoantenna, Thermal emission, Absorption, Plasmonics, Local Density of Optical States

1. INTRODUCTION

Several applications such as energy conversion,[1–3] gas detection,[4] or radiative cooling[5,6] requires a precise control of the thermal emission in the infrared. In recent decades, researchers have demonstrated incandescent sources that exhibit monochromatic, directional, and even fast modulated infrared emission.[7–13] Yet the modulation of thermal emission at a rate faster than a few hundreds of kHz is a further challenge that has not been achieved. It would be particularly useful for short range communications applications such as remote control or wireless LAN communication systems. According to Kirchhoff's law, thermal emission is the product of the absorptivity and the blackbody spectral radiance at the working temperature. Modulation of thermal emission can thus be obtained by dynamically tuning either the absorptivity of the device[14–16] or its temperature.[17] Electrical modulation of the emissivity of a stack of quantum wells has allowed modulating thermal emission at a record rate of 600 kHz.[16] However in this kind of device, the modulation speed is limited by parasitic resistances and capacitances in the semiconductor layers.

In order to reach higher modulation speeds we propose a novel approach that consists in heating only nanoscale volumes whose cooling times can be extremely fast.[18] Indeed, the thermal diffusion time constant of an object of size h is proportional to h^2/D, with D the thermal diffusion coefficient. Hence a cubic volume of matter with a 100 nm size has a characteristic diffusion time in the range of a few tens of nanoseconds – the diffusion coefficient being on the order of $10^{-6}\mathrm{m}^2.\mathrm{s}^{-1}$ for most non-metallic materials. Such short thermal timescales should enable modulation speeds as fast as a few tens of MHz.

emilie.sakat@c2n.upsaclay.fr
christophe.sauvan@institutoptique.fr

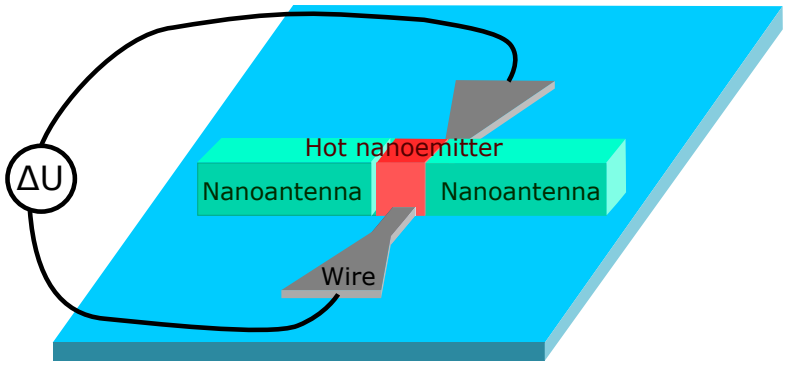

Figure 1. Device general principle: a cubic hot nanoemitter is inserted in the gap of a dimer nanoantenna and deposited on a substrate. The heating of the nanovolume can be obtained electrically with a metallic wire of varying width: the width is chosen narrower below the nanoemitter so that the electric resistance locally increases allowing to dissipate heat by Joule effect at this precise location.

However, the thermal emission in the infrared of these isolated and sub-wavelength nanoemitters is weak. To design their emission in a cold environment, a local Kirchhoff law has to be used due to the anisothermal nature of the proposed device: it indicates that the problem is equivalent to optimize the nanovolume absorption cross-section in its complex environment.[19] To compensate the weak absorption inside subwavelength objects, different strategies can be used. In particular, the absorber properties, the illumination, or the environment can be engineered. Many works have been dedicated to the optimization of the absorption by a single nanoparticle.[20–26] For an absorber in a homogeneous medium, the physical bounds of the problem are known; they depend on the multipolar character of the particle. The maximum absorption cross-section of a molecule or a nanoparticle that behaves like a pure electric dipole (dipolar approximation), is $3\lambda^2/(8\pi n^2)$, with λ the wavelength and n the surrounding refractive index.[20,23] This upper bound can only be reached if the absorber polarizability α matches a precise value, $\alpha_{\text{opt}} = i3\lambda^3/(8\pi^2 n)$. Subwavelength particles that go beyond the dipolar approximation offer additional degrees of freedom and are governed by different physical bound.[21–26] Plunging the absorber (or hot nanovolume) in a complex medium or modifying the illumination offers additional possibilities to tailor the absorption.[27,28] In this work, we consider a subwavelength hot nanovolume in a complex environment (inhomogeneous or not) as depicted in Fig. 1. According to the local Kirchhoff's law , we focus on the absorption inside the hot nanovolume and do not discuss dissipation in the surroundings, if any. To fully exploit the control possibilities offered by the environment, it is crucial to know what is the relevant figure of merit. The absorption density is proportional to the local electric-field intensity $|\mathbf{E}(\mathbf{r})|^2$,[29] which results from the environment *and* the absorber. It is highly desirable to decouple both contributions to provide a figure of merit that is intrinsic to the environment. Only then can we properly compare the ability of different structures to modify absorption.

In this work, we derive a general upper bound for the power dissipated in a subwavelength absorber (or equivalently the power emitted by a hot nanoemitter) surrounded by any complex inhomogeneous environment. Owing to its subwavelength dimensions, the absorber is treated in the electric-dipole approximation. On the other hand, the electromagnetic properties of the environment are treated rigorously without any approximation. The upper bound is independent of the absorber; it entirely depends on the environment and the illumination. Thus, it provides a relevant figure of merit for comparing the ability of different systems to enhance absorption (or thermal emission). This figure of merit results from the interplay between two electromagnetic properties of the environment, the field enhancement and the Green tensor. We also discuss under which conditions the system can reach the upper bound. This theoretical formalism is finally applied to the design of a high-speed modulation incandescent source. In particular, three kind of environments for the hot nanovolume are compared: a plasmonic dimer nanoresonator, a Yagi-Uda nanoantenna and a L-shape nanoantenna.

2. RESULTS

2.1 Kirchhoff's law applied to an anisothermal structure

In contrast to previous works, the approach proposed in this paper relies on the use of anisothermal structures where only nanoscale volumes are heated while the rest of the device remains at lower temperatures. The usual Kirchhoff's law is established for thermodynamic equilibrium and cannot predict thermal emission of complex structures composed of different parts at different temperatures. In this case, the theoretical study has to be realized in the framework of a generalized version of Kirchhoff's law. It is indeed possible to establish the equality between the *local* emission rate in one specific direction, wavelength and polarization and the *local* absorption rate for the same wavelength, polarization and direction for any finite-size body with arbitrary geometry.[19,30] In this generalized version of Kirchhoff's law applied to an anisothermal structure where only a small part is hot while the rest of the device is cold, the key physical quantity is the absorption cross-section. Since the temperature to be taken into account is the temperature at the point of interest, we have to consider the absorption cross-section associated to the hot nanovolume and not the cross-section of the whole structure. It is given by:

$$\sigma_{\mathrm{a}}(\mathbf{u},\omega) = \frac{\omega}{2P_0}\int_{V_e} \mathrm{Im}(\varepsilon)|\mathbf{E}|^2 d^3\mathbf{r}. \tag{1}$$

where ω is the frequency, P_0 is the norm of the Poynting vector of the incident plane wave, ε is the dielectric permittivity of the material, $\mathbf{E}$ is the total electric field and V_e is the volume of interest, i.e. the nanoscale volume that will be heated. We can define the local absorption cross section as:

$$\rho_{\mathrm{a}}(\mathbf{r},\mathbf{u},\omega) = \frac{\omega \mathrm{Im}(\varepsilon)|\mathbf{E}|^2}{2P_0}. \tag{2}$$

The power emitted by the hot nanovolume V_e is then given by:

$$P_e(\mathbf{u},\omega) = \int_{V_e} \rho_{\mathrm{a}}(\mathbf{r},\mathbf{u},\omega) I_B(\omega, T(\mathbf{r})) d^3\mathbf{r}. \tag{3}$$

where $I_B(\omega, T(\mathbf{r}))$ is the spectral radiance of a blackbody.[19,30]

If we assume a constant temperature in the nanovolume V_e, we obtain $P_e = \sigma_{\mathrm{a}} I_B(T)$. It evidences that in order to increase the extraction of thermal power from a given object, one needs to increase its absorption cross-section. Therefore in the following discussions, we focus on the calculation of σ_{a} given by Eq. 1. Hereafter, we refer to the volume V_e as the nanoemitter or as the absorber.

2.2 General considerations on absorption of a nanoparticle in a complex environment

Absorption by deeply-subwavelength and isolated objects is extremely weak. For instance, the absorption cross-section at $\lambda = 10$ μm of a small cube of silicon nitride with a 200 nm side is on the order of 0.01 μm^2, i.e. only one fourth of its geometrical surface. In order to take advantage of the short thermal timescales offered by small objects, we thus need to increase significantly the absorption in a given object whose typical size is on the order of 100 nm. In principle, the maximum absorption cross-section for a small object behaving as a pure electric dipole is $3\lambda^2/(8\pi) = 12$ μm^2 at $\lambda = 10$ μm. However, reaching this upper bound with a subwavelength nanosphere whose polarizability is given by the quasistatic limit requires the use of a material with a relative permittivity close to -2. In practice, obtaining an absorption cross-section of $3\lambda^2/(8\pi)$ at $\lambda = 10$ μm with a sphere of radius 100 nm in air requires to fill the nanosphere with a relative permittivity equal to -2.0095+0.0005i. Such a precise value is impossible to find with realistic materials. It has been shown recently that absorption cross-sections close to $3\lambda^2/(8\pi)$ or even larger can be obtained with realistic materials,[23] but with bigger objects that do not behave as pure electric dipoles and that would have longer thermal timescales.

Plunging the absorber (or hot nanovolume) in a complex medium or modifying the illumination offers additional possibilities to tailor the absorption.[27,28] To fully exploit the control possibilities offered by the environment, it is crucial to know what is the relevant figure of merit. Let us underline that the link between the thermal emission (or absorption) and the environment properties is more complex than the proportionality

relation between spontaneaous emission and LDOS. For an emitter coupled to a resonant cavity, the spontaneous emission enhancement has a well-known upper bound, the Purcell factor, which is intrinsic to the resonator and independent of the emitter.[31–33] The upper bound is reached if emitter and resonator fulfill a few matching conditions – spectral, spatial, and in polarization.[33]

In the case of absorption, let us start by the simple case where the absorber perturbs only slightly the electromagnetic field. In this perturbation regime, the Born approximation can be used and the field inside the absorber is asssumed to be equal to the field $\mathbf{E}_b$ provided by the environment alone, see Fig. 2b. In that case, the absorption is simply proportional to the field enhancement $|\mathbf{E}_b|^2/|\mathbf{E}_{\text{inc}}|^2$. Hence, hot spots are often thought to provide large absorption enhancements and nanoantennas are often engineered for maximizing the field enhancement they provide.[34,35] However, if the presence of the absorber significantly affects the local field, a perturbative treatment is not valid and the situation is more complex: the field enhancement is not the only electromagnetic property of the environment that drives the absorption. For instance, it has been recently shown that, in a scalar quasi-static case, the absorption cross-section is inversely proportional to the square of the LDOS .[27] The work in Ref.[27] considers absorption in a given system absorber + environment but does not decouple the contribution of the absorber from the impact of the environment. It does not study the physical bounds of the problem. Until now, no upper bound – kind of Purcell factor analogue – has been derived for the problem of an absorber in a complex environment.

Antenna theory provides a solution in one specific case. For an antenna receiving a signal from the direction (θ, ϕ), the maximum absorption cross-section of the load is $G_a(\theta,\phi)\lambda^2/(4\pi n^2)$, with G_a the antenna gain.[36–38] This upper bound is reached if the load is impedance-matched with the antenna. The gain is defined for an emitting antenna as the fraction of the wall-plug power radiated in the direction (θ, ϕ). Unfortunately, the $G_a\lambda^2/(4\pi n^2)$ limit only applies to plane-wave illumination and to antennas working in the scalar approximation when one component of the electromagnetic field is dominant. In cases where the vectorial nature of the electromagnetic field cannot be neglected, the problem remains open. Moreover, the antenna point of view highlights the gain, whereas other derivations underline the field enhancement and the LDOS.[27] It is thus important to generalize existing results, while enlightening the link between them.

2.3 Derivation of an upper bound for an absorber in any complex environment

We consider the problem illustrated in Fig. 2(a). An absorbing subwavelength particle (in red) is placed in a complex absorbing or non-absorbing environment (in green) and illuminated by an incident field $\mathbf{E}_{\text{inc}}$. We focus on the absorption inside the particle. We consider passive materials and use the $\exp(-i\omega t)$ convention for time-harmonic fields, with $\omega = 2\pi c/\lambda$. The following derivations apply to any incident field and any environment geometry. We refer to the environment as "the antenna", but no particular assumption is made on its geometry.

The total electric field can be written as $\mathbf{E}(\mathbf{r}) \equiv \mathbf{E}_b(\mathbf{r}) + \mathbf{E}_s(\mathbf{r})$, where $\mathbf{E}_b$ is the field *in the absence of* the absorber, see Fig. 2(b), and $\mathbf{E}_s$ is the field scattered by the absorber. It is the field radiated by the current source induced inside the absorber by the exciting field. We now make the sole assumption of our derivation. We

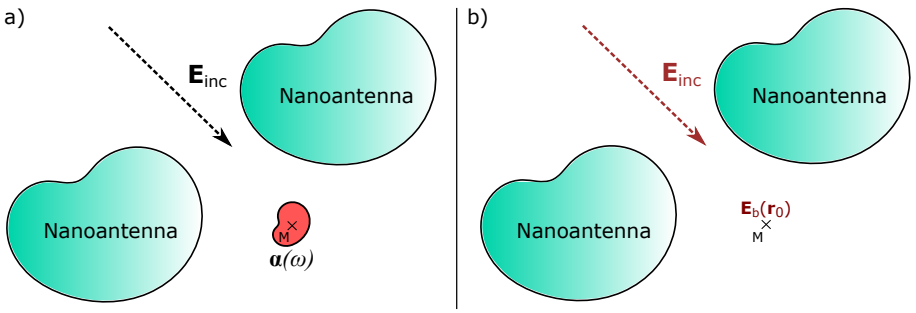

Figure 2. (a) Subwavelength absorber (in red) in an arbitrary environment (in green, referred to as "nanoantenna") illuminated by an incident field $\mathbf{E}_{\text{inc}}$. We focus on the absorption inside the particle. (b) Same problem without the absorber. The field $\mathbf{E}_b$ is the field scattered by the environment alone.

assume that the subwavelength particle scatters light like an electric dipole $\mathbf{p}$ located at $\mathbf{r} = \mathbf{r}_0$. The scattered field is then $\mathbf{E}_s(\mathbf{r}) = \mu_0\omega^2\mathbf{G}(\mathbf{r},\mathbf{r}_0)\mathbf{p}$, with $\mathbf{G}$ the Green tensor of the antenna alone.

The power dissipated in the particle is the difference between extinction and scattering, $P_a = P_e - P_s$.[29] Within the dipole approximation, $P_e = -\frac{1}{2}\omega\mathrm{Im}(\mathbf{p}^\dagger\mathbf{E}_b)$ and $P_s = \omega\mathbf{p}^\dagger\mathbf{g}\mathbf{p}$, with $\mathbf{g} \equiv \frac{1}{2}\mu_0\omega^2\mathrm{Im}[\mathbf{G}(\mathbf{r}_0,\mathbf{r}_0)]$ (see Appendix A). It follows

$$P_a = -\frac{1}{2}\omega\mathrm{Im}(\mathbf{p}^\dagger\mathbf{E}_b) - \omega\mathbf{p}^\dagger\mathbf{g}\mathbf{p}\,, \tag{4}$$

where $\mathbf{E}_b \equiv \mathbf{E}_b(\mathbf{r}_0)$ and $\mathbf{p}^\dagger$ is the conjugate transpose of $\mathbf{p}$. The induced dipole is $\mathbf{p} = \varepsilon_0\boldsymbol{\alpha}(\omega)[\mathbf{E}_b(\mathbf{r}_0) + \mu_0\omega^2\mathbf{S}(\mathbf{r}_0,\mathbf{r}_0)\mathbf{p}]$, with $\boldsymbol{\alpha}(\omega)$ the polarizability tensor of the particle and $\mathbf{S} = \mathbf{G} - \mathbf{G}_0$, $\mathbf{G}_0$ being the Green tensor of the homogeneous medium of refractive index n that surrounds the particle.

In order to derive an upper bound that is independent of the absorber, we calculate the maximum of $P_a = f(\mathbf{p})$. In a complex medium composed of passive materials, the quantity $\omega\mathbf{u}^\dagger\mathbf{g}\mathbf{u}$ gives the total electromagnetic power emitted by the electric-dipole source $\mathbf{u}$ (see Appendix A). Therefore, $\mathbf{u}^\dagger\mathbf{g}\mathbf{u} \geqslant 0$ whatever the vector $\mathbf{u}$ and $\mathbf{g}$ is a semi-definite positive matrix. We now use this important property to derive the maximum of $P_a = f(\mathbf{p})$. For that purpose, we have to rewrite the dissipated power under the form $P_a = -\omega\mathbf{u}^\dagger\mathbf{g}\mathbf{u} + A$, where A is independent of $\mathbf{p}$. A few algebraic manipulations of Eq. (4) lead to (details can be found in Appendix B)

$$P_a = -\omega\Big(\mathbf{p}^\dagger + \frac{i}{4}\mathbf{E}_b^\dagger\mathbf{g}^{-1}\Big)\mathbf{g}\Big(\mathbf{p} - \frac{i}{4}\mathbf{g}^{-1}\mathbf{E}_b\Big) + \frac{\omega}{16}\mathbf{E}_b^\dagger\mathbf{g}^{-1}\mathbf{E}_b. \tag{5}$$

Now the dissipated power takes the form $P_a = -\omega\mathbf{u}^\dagger\mathbf{g}\mathbf{u} + A$, with $\mathbf{u} = \mathbf{p} - \frac{i}{4}\mathbf{g}^{-1}\mathbf{E}_b$ and $A = \frac{\omega}{16}\mathbf{E}_b^\dagger\mathbf{g}^{-1}\mathbf{E}_b$. Since $\mathbf{g}$ is a semi-definite positive matrix, we know that $-\omega(\mathbf{p}^\dagger + \frac{i}{4}\mathbf{E}_b^\dagger\mathbf{g}^{-1})\mathbf{g}(\mathbf{p} - \frac{i}{4}\mathbf{g}^{-1}\mathbf{E}_b) \leqslant 0$. This readily leads to an upper bound for the absorption, which is independent of the absorber and depends only on the environment and the illumination, $P_a \leqslant P_a^{\max}$, with

$$P_a^{\max} = \frac{\omega}{16}\mathbf{E}_b^\dagger\mathbf{g}^{-1}\mathbf{E}_b\,. \tag{6}$$

According to Eq. (5), the upper bound is reached for an optimal dipole $\mathbf{p}_{\mathrm{opt}} = \frac{i}{4}\mathbf{g}^{-1}\mathbf{E}_b$. The optimal polarizability that yields the maximum absorption is then (see Appendix C)

$$\boldsymbol{\alpha}_{\mathrm{opt}}(\omega) = \frac{c^2}{\omega^2}\left[\mathbf{S}^*(\mathbf{r}_0,\mathbf{r}_0) - i\frac{\omega n}{3\pi c}\mathbf{I}\right]^{-1}. \tag{7}$$

with $\mathbf{S}^*$ the conjugate of $\mathbf{S}$. Any other polarizability in the same environment necessarily absorbs less light. Equation (7) can be seen as a vectorial generalization of the usual scalar impedance-matching concept.[36,39]

We define the absorption efficiency $\eta_a = P_a/P_{\mathrm{inc}}$ as the fraction of the incident power that is absorbed inside the particle. The maximum absorption efficiency is

$$\eta_a^{\max} = \frac{\omega}{16}\frac{\mathbf{E}_b^\dagger\mathbf{g}^{-1}\mathbf{E}_b}{P_{\mathrm{inc}}}. \tag{8}$$

If the incident field is a plane wave, we rather define a maximum absorption cross-section by normalizing $P_a^{\max}$ with the incident Poynting vector $\frac{1}{2}\varepsilon_0 cn|\mathbf{E}_{\mathrm{inc}}|^2$,

$$\sigma_a^{\max} = \frac{3\lambda^2}{8\pi n^2}g_0\frac{\mathbf{E}_b^\dagger\mathbf{g}^{-1}\mathbf{E}_b}{|\mathbf{E}_{\mathrm{inc}}|^2}, \tag{9}$$

where $g_0\mathbf{I} \equiv \frac{1}{2}\mu_0\omega^2\mathrm{Im}[\mathbf{G}_0(\mathbf{r}_0,\mathbf{r}_0)] = \omega^3 n/(12\pi\varepsilon_0 c^3)\mathbf{I}$. Note that, in a homogeneous environment, $\mathbf{g} = g_0\mathbf{I}$, $\mathbf{E}_b = \mathbf{E}_{\mathrm{inc}}$, and we recover the usual result $\sigma_a^{\max} = 3\lambda^2/(8\pi n^2)$.

Equations (6)-(9) form the central result of this article. They deserve a few comments before we illustrate their consequences on a couple of examples. The upper bound is independent of the absorber; it solely depends on the antenna and the incident field. Thus, Eqs. (8) and (9) provide meaningful figures of merit for comparing the ability of different systems to enhance absorption. These novel figures of merit result from an interplay between the local field $\mathbf{E}_b$ provided by the sole antenna and the imaginary part of its Green tensor $\mathbf{g}$.

In the case where the vectorial nature of the electromagnetic field can be neglected, the general upper bound can be replaced by an approximate form. Let us assume that the field $\mathbf{E}_b$ and the Green tensor $\mathbf{g}$ are dominated by a single component, the z component. Within this scalar approximation, Eq. (9) reduces to

$$\sigma_a^{\max} \approx \frac{3\lambda^2}{8\pi n^2} \frac{|E_{bz}|^2}{|E_{\text{inc}}|^2} \frac{g_0}{g_{zz}} = \frac{3\lambda^2}{8\pi n^2} \frac{\text{Intensity enh.}}{\text{LDOS enh.}} . \tag{10}$$

The upper bound appears to be the ratio between the intensity enhancement $|E_{bz}|^2/|E_{\text{inc}}|^2$ and the LDOS enhancement g_{zz}/g_0. The fact that a LDOS enhancement is detrimental can be intuitively understood as follows: a larger LDOS increases the radiation of the induced dipole, i.e., it increases the scattering at the expense of absorption.

It can be shown using reciprocity that Eq. (10) is equivalent to $\sigma_a^{\max} = G_a(\theta,\phi)\lambda^2/(4\pi n^2)$, with G_a the antenna gain.[40] The upper bound derived with antenna theory is thus a particular (scalar) case of the general result in Eq. (9). Two equivalent points of view can be adopted. They provide different conclusions and it is interesting to consider both of them. Equation (10) evidences that antennas supporting hot spots are a good choice if, *and only if*, the formation of hot spots is not concomitant with a large LDOS. On the other hand, the antenna gain is the product of the radiative efficiency and the directivity, $G_a(\theta,\phi) = \eta_r D(\theta,\phi)$.[36] This second point of view underlines that (i) directional structures perform better and (ii) dielectric objects ($\eta_r = 1$) are better choices than plasmonic structures with $\eta_r < 1$.

2.4 Comparison of three kind of environments

Let us illustrate the theory with a few examples. First, we study a plasmonic dimer nanoresonator and a Yagi-Uda antenna made of silicon nanospheres. Both can be treated in the scalar approximation. Secondly, we consider a structure that can only be studied with a fully vectorial formalism: silicon nanospheres in a L-shape configuration.

In the case of a single-mode antenna, LDOS and field enhancement are not independent since both are driven by the excitation of an eigenmode.[42] Both are resonant with the same spectral profile and increasing one necessarily enhances the other. Thus, quite counter-intuitively, the value of the upper bound in Eq. (10) *is not correlated to the presence of hot spots*. To illustrate this conclusion, let us consider a dimer made of two gold nanorods (length 414 nm, radius 15 nm, and gap 20 nm) illuminated by a normal-incident plane wave. Only the dipole mode at $\lambda = 3$ μm is excited. Figure 3(a) displays the spectra of the maximum absorption cross-section and the intensity enhancement at the gap center: $|\mathbf{E}_b|^2/|\mathbf{E}_{\text{inc}}|^2$ is resonant whereas $\sigma_a^{\max}$ is not (even if it is not shown here the LDOS enhancement is resonant at the same wavelength than the intensity enhancement). For comparison with the upper bound of an optimal absorber in a homogeneous medium, we plot the ratio of the maximum absorption cross-section, $\sigma_a^{\max}$ with $3\lambda^2/(8\pi n^2)$. This ratio being always ¡ 1 any absorber in the gap of this particular plasmonic dimer absorbs less than an optimal absorber in a homogeneous medium. Figure 3(b) shows the variation of $|\mathbf{E}_b|^2/|\mathbf{E}_{\text{inc}}|^2$ and the ratio of $\sigma_a^{\max}$ and $3\lambda^2/(8\pi n^2)$ with w. As w is varied, the cylinder length is tuned to keep the resonance fixed at $\lambda = 3$ μm so that all the antennas are at resonance. The maximum absorption cross-section only weakly varies while the field enhancement strongly decreases.

Since the upper bound in the scalar case is proportional to the radiative efficiency η_r and the directivity, we switch to a Yagi-Uda antenna made of silicon nanospheres, which is known to be directional.[44] We keep a plane-wave illumination and a wavelength of $\lambda = 3$ μm. The silicon is transparent and $\eta_r = 1$. The maximum absorption cross-section $\sigma_a^{\max}$ is represented on Fig. 4(a) as a function of the incident angle θ for $\mathbf{r}_0$ located in between the reflector and the first director. The incident plane wave is either TM (black curve) or TE (red curve) polarized. For $\theta = 0°$, $\sigma_a^{\max}$ is one order of magnitude larger than $3\lambda^2/(8\pi n^2)$. This evidences that a dielectric directional antenna can provide larger absorption enhancements than a plasmonic antenna supporting

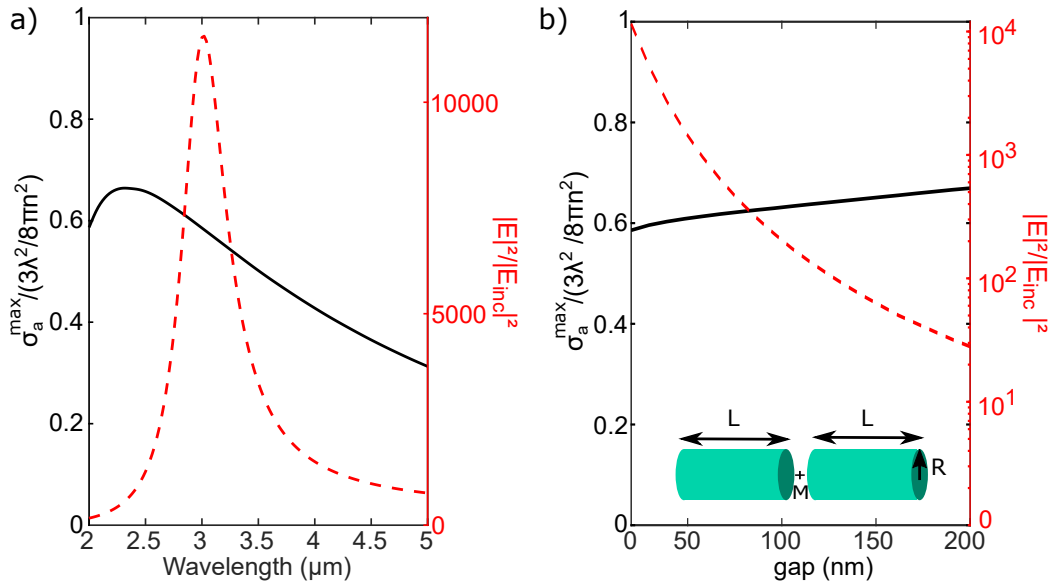

Figure 3. Nanoantennas in the scalar approximation. Dimer composed of two gold cylinders illuminated by a normal-incident plane wave polarized along the cylinder axis. The point $M(\mathbf{r}_0)$ is the gap center. (a) Spectra of the maximum absorption cross-section $\sigma_a^{\max}$ (left axis, black curve) and the intensity enhancement (right axis, dashed red curve) for $L=414$ nm, $R=15$ nm, and $w=20$ nm. (b) Maximum absorption cross-section and intensity enhancement as a function of the gap width w (the cylinder length is tuned to keep the resonance fixed at $\lambda=3$ μm). Calculations are performed with an aperiodic Fourier modal method dedicated to body-of-revolution objects.[41] The antenna is embedded in a medium of refractive index $n=1.5$.

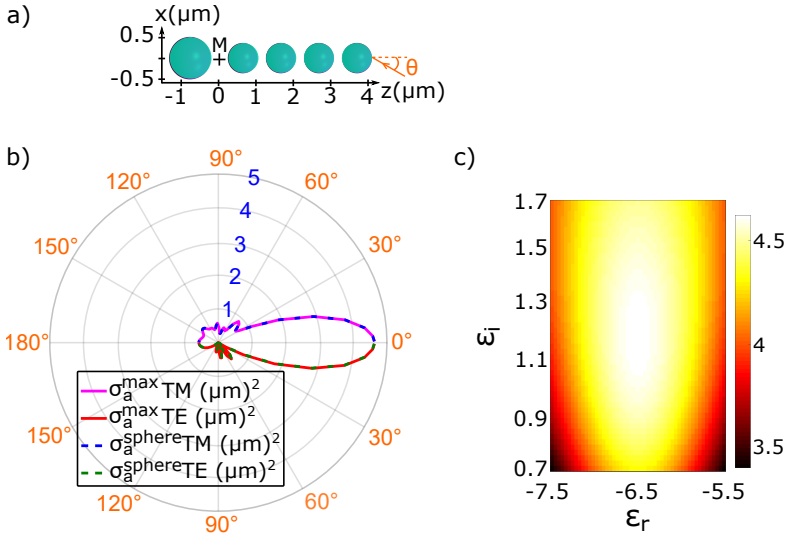

Figure 4. (a) Nanoantennas in the scalar approximation. Yagi-Uda antenna composed of silicon spheres (refractive index 3.436). The reflector (radius 498 nm) is separated from the first director by 700 nm (green spheres). The four directors (radius 382 nm) are equally spaced by 250 nm. The point $M(\mathbf{r}_0)$ is the center between the reflector and the first director. (b) Maximum absorption cross-section $\sigma_a^{\max}$ at $\lambda=3$ μm as a function of the incident angle θ for a TM (purple curve) or TE (red curve) polarized plane wave. Direct absorption cross-section calculation for an absorbing nanosphere (radius 176 nm and permittivity ε_{opt}=-6.46+1.22i) inserted inside the non-absorbing Yagi-Uda antenna. The blue squares curve corresponds to TM polarization and the green squares curve to TE polarization. These rigorous calculations are superimposed on the upper bound (no absorber, Yagi-Uda antenna alone). (c) Direct absorption cross-section of an absorbing nanosphere of radius 176 nm inserted at $\mathbf{r}_0$. The real and imaginary parts of the absorber permittivity are varied around the optimal value ε_{opt}=-6.46+1.22i. Calculations are performed with a rigorous multipole method.[43,44] The antenna is embedded in a medium of refractive index $n=1.5$.

hot spots. Note that, for a fixed geometry, the upper bound changes with the incident angle, whereas the optimal polarizability given by Eq. (7) is constant. Once the polarizability has been chosen, one is sure to reach the upper bound whatever the incident angle.

Before considering fully vectorial examples, we discuss the possibility to reach the upper bound on the Yagi-Uda example. The optimal polarizability corresponds for instance to a sphere of radius 176 nm filled with a material of relative permittivity $\varepsilon_{\text{opt}} = -6.46 + 1.22i$; the relation between the electric-dipole polarizability, the sphere radius, and the permittivity has been rigorously calculated with Mie theory. Such a permittivity at λ=3 μm can be obtained with highly-doped semiconductor nanocrystals.[45,46] We have checked with a rigorous numerical method that inserting this nanosphere in the Yagi-Uda antenna yields an absorption that is indeed equal to the upper bound (see Figure 4(b)). We have also tested the robustness of the optimal polarizability. Figure 4(c) shows the absorption cross-section at normal incidence in TM polarization obtained by varying the absorber permittivity around the optimum. Since the cross-section varies smoothly around the maximum, we have a good flexibility on the choice of the permittivity.

Let us now consider a L-shape antenna made of three silicon spheres, see Figs. 5(a)-(b). Such a structure cannot be described in the scalar approximation, especially for positions $\mathbf{r}_0$ outside the symmetry planes. In that case, Eq. (10) is not valid. The system can only be characterized by the vectorial upper bound of Eq. (9). The latter depends on the absorber position and it is important, for a given nanoantenna, to evaluate where the particle could reach the best absorption. Figures 5(a)-(b) show respectively the spatial distributions of the intensity enhancement and the maximum absorption cross-section in the (x, y) plane for z = 232 nm. The antenna is illuminated from the bottom by a plane wave propagating along the z axis and polarized linearly along the white arrow. The blue cross in Fig. 5(b) marks the position where the upper bound is maximum. It does not correspond to the maximum of $|\mathbf{E}_b|^2/|\mathbf{E}_{\text{inc}}|^2$, which evidences, once again, that seeking hot spots is not sufficient to maximize the absorption.

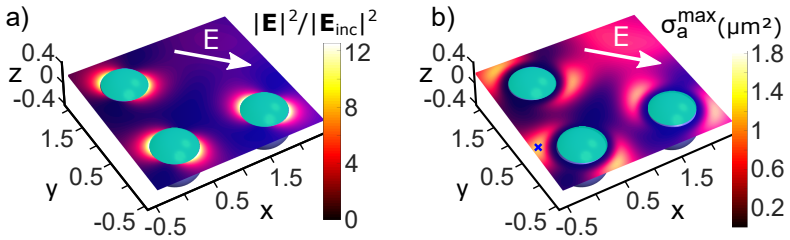

Figure 5. Beyond scalar approximation. L-shape antenna made of three silicon spheres (radius 430 nm) equally spaced by 1.54 μm and embedded in a medium of index n = 1.5 at λ = 3 μm. (a) Intensity enhancement and (b) maximum absorption cross-section as a function of the position $\mathbf{r}_0$ in the (x, y) plane for z = 232 nm. The map of the intensity enhancement is clearly different from the spatial distribution of the maximum absorption cross-section. Calculations are performed with a rigorous multipole method.[43,44]

This study shows that the realization of an efficient high-speed modulation incandescent source based on the approach presented in Fig. 1 is possible. An array of highly-doped semiconductor nanoparticles that would be heated locally and inserted in the vicinity of cold nanoantennas (Yagi-Uda nanoantennas appear to be a good choice) shall be suited to the realization of such device.

3. CONCLUSION

In conclusion, we derived an upper bound for the problem of absorption by a dipolar absorber in a complex environment, homogeneous or not. The derivation relies on a vectorial formalism and is valid for any environment and any illumination. Since it decouples the environment from the absorber, the upper bound provides a meaningful figure of merit for comparing the intrinsic ability of different structures to enhance absorption in a nanovolume. Moreover, it allows seeking, for one given structure, the optimal position for the absorber. In the scalar approximation, the relevant parameter is not the field enhancement but the ratio between field enhancement and LDOS. Thus, although placing an absorber in a hotspot of a plasmonic structure can increase the absorption,[18] plasmonic antennas supporting hot spots are not necessarily the best candidates to reach

high absorption enhancements. Larger enhancements can be achieved with dielectric directional antennas. In cases where the scalar approximation is not valid or the illumination is not a plane wave, the situation is more complex and our general upper bound is the good figure of merit to characterize the problem. Since it relies on electromagnetic calculations (field enhancement and Green tensor) that are nowadays performed routinely, we think that this work opens new avenues for understanding and optimizing absorption in subwavelength volumes inserted in complex media. This result opens the way to the realization of an efficient device composed of arrays of nanoemitters that would be heated locally and inserted in the vicinity of cold nanoantennas allowing a high modulation rate together with an enhanced thermal emission. Moreover various kind of nanoantennas can be placed on the metasurface allowing to tune actively the emission of the nanoemitter in directivity, wavelength and polarization by heating specifically the emitters related to one antenna or the other. This approach will enable the design of cheap, compact and dynamic IR sources. Furthermore given the generality of the derived upper bound, it should also benefit others applications based on light absorption in several spectral domains: SEIRA, photovoltaics, or nanochemistry.

APPENDIX A. DEMONSTRATION OF THE POWER DISSIPATED BY A DIPOLAR ABSORBER

Equation (4) of the main text gives the power dissipated in a dipolar absorber plunged in a complex environment and illuminated by an incident field. The absorption is expressed as the difference between the extinction and the scattered power. It is a classical expression but we present its derivation here for the sake of completeness. In contrast to the standard demonstration that can be found in some textbooks, we provide a derivation that carefully handles the singularity of the field radiated by a dipole source on itself.

Energy conservation implies that the flux of the Poynting vector through a closed surface Σ surrounding the absorber (and only the absorber) is negative and equal to the opposite of the power P_a dissipated inside Σ,

$$P_a = -\iint_{\Sigma} \frac{1}{2}\mathrm{Re}(\mathbf{E}^* \times \mathbf{H}) \cdot d\mathbf{S}, \tag{11}$$

where $\mathbf{E}$ and $\mathbf{H}$ are the total electric and magnetic fields and $\mathbf{E}^*$ is the conjugate of $\mathbf{E}$. Usually, the total field is separated in two contributions, $\mathbf{E}(\mathbf{r}) = \mathbf{E}_b(\mathbf{r}) + \mathbf{E}_s(\mathbf{r})$, where $\mathbf{E}_b$ is the field *in the absence of* the absorber and $\mathbf{E}_s$ is the field scattered by the absorber located at $\mathbf{r} = \mathbf{r}_0$. By doing so, the dissipated power given by Eq. (11) can be expressed as the sum of two surface integrals. The first one corresponds to the extinction; it is given by $\iint_\Sigma \frac{1}{2}\mathrm{Re}(\mathbf{E}_s^* \times \mathbf{H}_b + \mathbf{E}_b^* \times \mathbf{H}_s) \cdot d\mathbf{S}$. The second integral corresponds to the power scattered by the absorber in the presence of the environment; it is given by $\iint_\Sigma \frac{1}{2}\mathrm{Re}(\mathbf{E}_s^* \times \mathbf{H}_s) \cdot d\mathbf{S}$. The latter corresponds to the power emitted by the induced dipole $\mathbf{p}$ since $\mathbf{E}_s(\mathbf{r}) = \mu_0\omega^2\mathbf{G}(\mathbf{r}, \mathbf{r}_0)\mathbf{p}$, with $\mathbf{G}(\mathbf{r}, \mathbf{r}_0)$ the Green tensor of the environment. This power can be expressed as a function of the imaginary part of $\mathbf{G}(\mathbf{r}_0, \mathbf{r}_0)$. However, such derivation is not straightforward if one wants to properly handle the singularity of the real part of $\mathbf{G}(\mathbf{r}_0, \mathbf{r}_0)$.

In order to avoid the mathematical difficulty related to the Green tensor singularity, we present here a derivation that is based on a different decomposition of the total field. We write the total field as $\mathbf{E}(\mathbf{r}) = \mathbf{E}_0(\mathbf{r}) + \mathbf{E}_r(\mathbf{r})$, where $\mathbf{E}_0(\mathbf{r}) = \mu_0\omega^2\mathbf{G}_0(\mathbf{r}, \mathbf{r}_0)\mathbf{p}$ is the field radiated by the induced dipole $\mathbf{p}$ *in an homogeneous medium of refractive index* n and $\mathbf{E}_r(\mathbf{r}) = \mathbf{E}_b(\mathbf{r}) + \mu_0\omega^2\mathbf{S}(\mathbf{r}, \mathbf{r}_0)\mathbf{p}$, with $\mathbf{S} = \mathbf{G} - \mathbf{G}_0$. The field $\mathbf{E}_0(\mathbf{r})$ is singular at $\mathbf{r} = \mathbf{r}_0$, while the field $\mathbf{E}_r(\mathbf{r})$ is regular everywhere in Σ. The dissipated power can be written as

$$P_a = -\iint_{\Sigma} \frac{1}{2}\mathrm{Re}\big[(\mathbf{E}_r^* + \mathbf{E}_0^*) \times (\mathbf{H}_r + \mathbf{H}_0)\big] \cdot d\mathbf{S} \tag{12}$$

$$= -\iint_{\Sigma} \frac{1}{2}\Big[\mathrm{Re}(\mathbf{E}_r^* \times \mathbf{H}_r) + \mathrm{Re}(\mathbf{E}_0^* \times \mathbf{H}_0) + \mathrm{Re}(\mathbf{E}_r^* \times \mathbf{H}_0 + \mathbf{E}_0^* \times \mathbf{H}_r)\Big] \cdot d\mathbf{S}\,. \tag{13}$$

The dissipated power is the sum of three different terms. Let us have a look at the first two terms:

- $\iint_\Sigma \frac{1}{2}\mathrm{Re}(\mathbf{E}_r^* \times \mathbf{H}_r) \cdot d\mathbf{S} = 0$ since $\mathbf{E}_r$ and $\mathbf{H}_r$ verify Maxwell's equations without source inside Σ.

- $\iint_\Sigma \frac{1}{2}\mathrm{Re}(\mathbf{E}_0^* \times \mathbf{H}_0) \cdot d\mathbf{S}$ is the power emitted by the dipole source $\mathbf{p}$ in a homogeneous medium of refractive index n. It is given by the Larmor formula $\iint_\Sigma \frac{1}{2}\mathrm{Re}(\mathbf{E}_0^* \times \mathbf{H}_0) \cdot d\mathbf{S} = \frac{\omega^4 n}{12\pi\varepsilon_0 c^3}|\mathbf{p}|^2$. Since the imaginary part of the bulk Green tensor is given by $\mathrm{Im}[\mathbf{G}_0(\mathbf{r}_0,\mathbf{r}_0)] = n\frac{\omega}{6\pi c}\mathbf{I}$, we can write $\iint_\Sigma \frac{1}{2}\mathrm{Re}(\mathbf{E}_0^* \times \mathbf{H}_0) \cdot d\mathbf{S} = \frac{1}{2}\mu_0\omega^3 \mathbf{p}^\dagger \mathrm{Im}[\mathbf{G}_0(\mathbf{r}_0,\mathbf{r}_0)]\mathbf{p}$.

Now let us consider the third term in Eq. (4). We use the Lorentz reciprocity formula, which relates two time-harmonic solutions of Maxwell's equations $(\mathbf{E}_1, \mathbf{H}_1, \omega_1, \mathbf{j}_1)$ and $(\mathbf{E}_2, \mathbf{H}_2, \omega_2, \mathbf{j}_2)$, where $(\mathbf{E}_i, \mathbf{H}_i)$ is the electromagnetic field created by the current distribution $\mathbf{j}_i$ at the frequency ω_i. A general form of Lorentz reciprocity formula and its derivation can be found for instance in Annex 3 of Ref.[42] Here we consider two solutions of Maxwell's equations inside the closed surface Σ at the same frequency $\omega_1 = \omega_2 = \omega$. As the first solution, we consider the field $(\mathbf{E}_0, \mathbf{H}_0)$ radiated by the dipole $\mathbf{p}$, i.e., a current distribution $\mathbf{j}_1 = -i\omega\mathbf{p}\delta(\mathbf{r} - \mathbf{r}_0)$. As the second solution, we consider the regular field $(\mathbf{E}_r^*, -\mathbf{H}_r^*)$ that is solution to Maxwell's equations without source, i.e., a current distribution $\mathbf{j}_2 = 0$. We obtain (see Annex 3 of Ref.[42])

$$\iint_\Sigma \Big[(\mathbf{E}_r^* \times \mathbf{H}_0 + \mathbf{E}_0 \times \mathbf{H}_r^*)\Big] \cdot d\mathbf{S} = i\omega \mathbf{E}_r(\mathbf{r}_0)^\dagger \mathbf{p}, \tag{14}$$

where the superscript † denotes the conjugate transpose. One can then deduce the real part of this expression that takes the following form

$$\iint_\Sigma \mathrm{Re}\big(\mathbf{E}_r^* \times \mathbf{H}_0 + \mathbf{E}_0^* \times \mathbf{H}_r\big) \cdot d\mathbf{S} = -\omega \mathrm{Im}[\mathbf{E}_r(\mathbf{r}_0)^\dagger \mathbf{p}] = \omega \mathrm{Im}[\mathbf{p}^\dagger \mathbf{E}_r(\mathbf{r}_0)] \tag{15}$$

Finally, the power dissipated in the dipolar absorber becomes

$$P_a = -\frac{1}{2}\omega \mathrm{Im}[\mathbf{p}^\dagger \mathbf{E}_r(\mathbf{r}_0)] - \frac{1}{2}\mu_0\omega^3 \mathbf{p}^\dagger \mathrm{Im}[\mathbf{G}_0(\mathbf{r}_0,\mathbf{r}_0)]\mathbf{p}, \tag{16}$$

with $\mathbf{E}_r(\mathbf{r}_0) = \mathbf{E}_b(\mathbf{r}_0) + \mu_0\omega^2 \mathbf{S}(\mathbf{r}_0,\mathbf{r}_0)\mathbf{p}$ and $\mathbf{S} = \mathbf{G} - \mathbf{G}_0$. Thus, it follows

$$P_a = -\frac{1}{2}\omega \mathrm{Im}[\mathbf{p}^\dagger \mathbf{E}_b(\mathbf{r}_0)] - \frac{1}{2}\mu_0\omega^3 \mathrm{Im}[\mathbf{p}^\dagger \mathbf{S}(\mathbf{r}_0,\mathbf{r}_0)\mathbf{p}] - \frac{1}{2}\mu_0\omega^3 \mathbf{p}^\dagger \mathrm{Im}[\mathbf{G}_0(\mathbf{r}_0,\mathbf{r}_0)]\mathbf{p}. \tag{17}$$

By using the relation $\mathrm{Im}(\mathbf{p}^\dagger \mathbf{S}\mathbf{p}) = \frac{1}{2i}\big(\mathbf{p}^\dagger \mathbf{S}\mathbf{p} - \mathbf{p}^\dagger \mathbf{S}^\dagger \mathbf{p}\big) = \mathbf{p}^\dagger \frac{\mathbf{S}-\mathbf{S}^\dagger}{2i}\mathbf{p}$, we can write the dissipated power as

$$P_a = -\frac{1}{2}\omega \mathrm{Im}[\mathbf{p}^\dagger \mathbf{E}_b(\mathbf{r}_0)] - \omega \mathbf{p}^\dagger \mathbf{s}\mathbf{p} - \frac{1}{2}\mu_0\omega^3 \mathbf{p}^\dagger \mathrm{Im}[\mathbf{G}_0(\mathbf{r}_0,\mathbf{r}_0)]\mathbf{p}, \tag{18}$$

with $\mathbf{s} = \frac{1}{2}\mu_0\omega^2 \frac{\mathbf{S}(\mathbf{r}_0,\mathbf{r}_0) - \mathbf{S}(\mathbf{r}_0,\mathbf{r}_0)^\dagger}{2i}$.
Therefore, by defining the matrix $\mathbf{g}$ as $\mathbf{g} = \mathbf{s} + \frac{1}{2}\mu_0\omega^2 \mathrm{Im}[\mathbf{G}_0(\mathbf{r}_0,\mathbf{r}_0)] = \mathbf{s} + g_0\mathbf{I}$, we can express the power dissipated by the dipolar absorber as [see Eq. (4) in the main text]

$$P_a = -\frac{1}{2}\omega \mathrm{Im}[\mathbf{p}^\dagger \mathbf{E}_b(\mathbf{r}_0)] - \omega \mathbf{p}^\dagger \mathbf{g}\mathbf{p}\,. \tag{19}$$

Note that, in the case where the materials composing the environment are reciprocal, the tensors $\mathbf{G}$ and $\mathbf{S}$ are symmetric. Thus, the expressions of $\mathbf{g}$ and $\mathbf{s}$ can be simplified as $\mathbf{s} = \frac{1}{2}\mu_0\omega^2 \frac{\mathbf{S}(\mathbf{r}_0,\mathbf{r}_0) - \mathbf{S}(\mathbf{r}_0,\mathbf{r}_0)^*}{2i} = \frac{1}{2}\mu_0\omega^2 \mathrm{Im}[\mathbf{S}(\mathbf{r}_0,\mathbf{r}_0)]$ and $\mathbf{g} = \frac{1}{2}\mu_0\omega^2 \mathrm{Im}[\mathbf{G}(\mathbf{r}_0,\mathbf{r}_0)]$. We emphasize that the equations presented in the main text are valid for non-reciprocal materials, provided that $\mathbf{g}$ is properly defined.

APPENDIX B. DETAILS ON THE DERIVATION OF THE UPPER BOUND

The power dissipated in a dipolar absorber is given by Eq. (4). As explained in the main text, in order to derive an upper bound that is independent of the absorber, we have to rewrite the dissipated power under the form $P_a = -\omega \mathbf{u}^\dagger \mathbf{g} \mathbf{u} + A$, where A is independent of $\mathbf{p}$.

This can be done with the following algebraic manipulations:

$$\begin{aligned}
P_a &= -\omega \mathbf{p}^\dagger \mathbf{g} \mathbf{p} - \frac{1}{2}\omega \mathrm{Im}(\mathbf{p}^\dagger \mathbf{E}_b) = -\omega \mathbf{p}^\dagger \mathbf{g} \mathbf{p} + \frac{1}{4i}\omega \left(\mathbf{E}_b^\dagger \mathbf{p} - \mathbf{p}^\dagger \mathbf{E}_b \right) \\
&= -\omega \mathbf{p}^\dagger \mathbf{g} \mathbf{p} + \frac{1}{4i}\omega \left(\mathbf{E}_b^\dagger \mathbf{g}^{-1} \mathbf{g} \mathbf{p} - \mathbf{p}^\dagger \mathbf{g} \mathbf{g}^{-1} \mathbf{E}_b \right) \\
&= -\omega \left(\mathbf{p}^\dagger \mathbf{g} \mathbf{p} + \frac{i}{4} \mathbf{E}_b^\dagger \mathbf{g}^{-1} \mathbf{g} \mathbf{p} - \frac{i}{4} \mathbf{p}^\dagger \mathbf{g} \mathbf{g}^{-1} \mathbf{E}_b \right) \\
&= -\omega \left[\left(\mathbf{p}^\dagger + \frac{i}{4} \mathbf{E}_b^\dagger \mathbf{g}^{-1} \right) \mathbf{g} \mathbf{p} - \mathbf{p}^\dagger \mathbf{g} \frac{i}{4} \mathbf{g}^{-1} \mathbf{E}_b - \frac{i}{4} \mathbf{E}_b^\dagger \mathbf{g}^{-1} \mathbf{g} \frac{i}{4} \mathbf{g}^{-1} \mathbf{E}_b + \frac{i}{4} \mathbf{E}_b^\dagger \mathbf{g}^{-1} \mathbf{g} \frac{i}{4} \mathbf{g}^{-1} \mathbf{E}_b \right] \\
&= -\omega \left[\left(\mathbf{p}^\dagger + \frac{i}{4} \mathbf{E}_b^\dagger \mathbf{g}^{-1} \right) \mathbf{g} \mathbf{p} - \left(\mathbf{p}^\dagger + \frac{i}{4} \mathbf{E}_b^\dagger \mathbf{g}^{-1} \right) \mathbf{g} \frac{i}{4} \mathbf{g}^{-1} \mathbf{E}_b - \frac{1}{16} \mathbf{E}_b^\dagger \mathbf{g}^{-1} \mathbf{E}_b \right] \\
&= -\omega \left(\mathbf{p}^\dagger + \frac{i}{4} \mathbf{E}_b^\dagger \mathbf{g}^{-1} \right) \mathbf{g} \left(\mathbf{p} - \frac{i}{4} \mathbf{g}^{-1} \mathbf{E}_b \right) + \frac{\omega}{16} \mathbf{E}_b^\dagger \mathbf{g}^{-1} \mathbf{E}_b \,. \qquad (20)
\end{aligned}$$

APPENDIX C. DETAILED DERIVATION OF THE OPTIMAL POLARIZABILITY

We provide in this Section more details on the derivation of the optimal polarizability $\boldsymbol{\alpha}_{\mathrm{opt}}$ given by Eq. 7 in the main text. According to Eq. 5 in the main text, the maximum absorption is reached for an optimal dipole

$$\mathbf{p}_{\mathrm{opt}} = \frac{i}{4} \mathbf{g}^{-1} \mathbf{E}_b \,. \qquad (21)$$

The induced dipole, located at $\mathbf{r} = \mathbf{r}_0$, is given by

$$\mathbf{p} = \varepsilon_0 \boldsymbol{\alpha}(\omega) \left[\mathbf{E}_b + \mu_0 \omega^2 \mathbf{S}(\mathbf{r}_0, \mathbf{r}_0) \mathbf{p} \right] , \qquad (22)$$

where $\boldsymbol{\alpha}(\omega)$ is the polarizability tensor of the dipolar absorbing particle and $\mathbf{S} = \mathbf{G} - \mathbf{G}_0$, with $\mathbf{G}$ the Green tensor of the environment (without absorber) and $\mathbf{G}_0$ the Green tensor of the homogeneous medium of refractive index n that surrounds the particle.

By injecting Eq. (21) into Eq. (22), one finds that, in order to reach the upper bound, the absorber polarizability tensor has to fulfill the expression

$$\frac{i}{4} \mathbf{g}^{-1} = \varepsilon_0 \boldsymbol{\alpha}_{\mathrm{opt}}(\omega) \left[\mathbf{I} + \mu_0 \omega^2 \mathbf{S}(\mathbf{r}_0, \mathbf{r}_0) \frac{i}{4} \mathbf{g}^{-1} \right] . \qquad (23)$$

Right multiplying both sides of the equation by $-4i\mathbf{g}$ and isolating the polarizability leads to

$$\boldsymbol{\alpha}_{\mathrm{opt}}(\omega) = \mu_0 c^2 \left[\mu_0 \omega^2 \mathbf{S}(\mathbf{r}_0, \mathbf{r}_0) - 4i\mathbf{g} \right]^{-1} . \qquad (24)$$

Since, in the case of reciprocal materials, $\mathbf{g} = \frac{1}{2}\mu_0\omega^2 \mathrm{Im}[\mathbf{G}(\mathbf{r}_0, \mathbf{r}_0)] = \frac{1}{2}\mu_0\omega^2 \mathrm{Im}[\mathbf{G}_0(\mathbf{r}_0, \mathbf{r}_0)] + \frac{1}{2}\mu_0\omega^2 \mathrm{Im}[\mathbf{S}(\mathbf{r}_0, \mathbf{r}_0)] = \frac{\omega^3 n}{12\pi\varepsilon_0 c^3}\mathbf{I} + \frac{1}{2}\mu_0\omega^2 \mathrm{Im}[\mathbf{S}(\mathbf{r}_0, \mathbf{r}_0)]$, we have the following relation

$$\begin{aligned}
\mu_0 \omega^2 \mathbf{S}(\mathbf{r}_0, \mathbf{r}_0) - 4i\mathbf{g} =& \mu_0 \omega^2 \mathbf{S}(\mathbf{r}_0, \mathbf{r}_0) - 2i\mu_0 \omega^2 \mathrm{Im}[\mathbf{S}(\mathbf{r}_0, \mathbf{r}_0)] - i \frac{\omega^3 n}{3\pi\varepsilon_0 c^3} \mathbf{I} \\
=& \mu_0 \omega^2 \mathbf{S}^*(\mathbf{r}_0, \mathbf{r}_0) - i \frac{\omega^3 n}{3\pi\varepsilon_0 c^3} \mathbf{I} \,,
\end{aligned}$$

with $\mathbf{S}^*$ the conjugate of $\mathbf{S}$. Therefore, the optimal polarizability given by Eq. (24) can be rewritten as

$$\boldsymbol{\alpha}_{\mathrm{opt}}(\omega) = \mu_0 c^2 \left[\mu_0 \omega^2 \mathbf{S}^*(\mathbf{r}_0, \mathbf{r}_0) - i\frac{\omega^3 n}{3\pi\varepsilon_0 c^3}\mathbf{I}\right]^{-1}, \tag{25}$$

which is equivalent to Eq. 7 in the main paper,

$$\boldsymbol{\alpha}_{\mathrm{opt}}(\omega) = \frac{c^2}{\omega^2}\left[\mathbf{S}^*(\mathbf{r}_0, \mathbf{r}_0) - i\frac{\omega n}{3\pi c}\mathbf{I}\right]^{-1}. \tag{26}$$

Note that, in the case of non-reciprocal materials, the conjugate $\mathbf{S}^*$ has simply to be replaced by the conjugate transpose $\mathbf{S}^\dagger$.

REFERENCES

[1] Boriskina, S. V., Green, M. A., Catchpole, K., Yablonovitch, E., Beard, M. C., Okada, Y., Lany, S., Gershon, T., Zakutayev, A., Tahersima, M. H., Sorger, V. J., Naughton, M. J., Kempa, K., Dagenais, M., Yao, Y., Xu, L., Sheng, X., Bronstein, N. D., Rogers, J. A., Alivisatos, A. P., Nuzzo, R. G., Gordon, J. M., Wu, D. M., Wisser, M. D., Salleo, A., Dionne, J., Bermel, P., Greffet, J.-J., Celanovic, I., Soljacic, M., Manor, A., Rotschild, C., Raman, A., Zhu, L., Fan, S., and Chen, G., "Roadmap on optical energy conversion," *Journal of Optics* **18**(7), 073004 (2016).

[2] Rephaeli, E. and Fan, S., "Absorber and emitter for solar thermo-photovoltaic systems to achieve efficiency exceeding the shockley-queisser limit," *Opt. Express* **17**, 15145–15159 (Aug 2009).

[3] Lenert, A., Bierman, D. M., Nam, Y., Chan, W. R., Celanovic, I., Soljacic, M., and Wang, E. N., "A nanophotonic solar thermophotovoltaic device," *Nat Nano* **9**, 126–130 (Feb. 2014).

[4] Costantini, D., Lefebvre, A., Coutrot, A.-L., Moldovan-Doyen, I., Hugonin, J.-P., Boutami, S., Marquier, F., Benisty, H., and Greffet, J.-J., "Plasmonic metasurface for directional and frequency-selective thermal emission," *Phys. Rev. Applied* **4**, 014023 (Jul 2015).

[5] Chen, Z., Zhu, L., Raman, A., and Fan, S., "Radiative cooling to deep sub-freezing temperatures through a 24-h day-night cycle," *Nature Communications* **7**, 13729 (Dec. 2016).

[6] Liu, T. and Takahara, J., "Ultrabroadband absorber based on single-sized embedded metal-dielectric-metal structures and application of radiative cooling," *Opt. Express* **25**, A612–A627 (Jun 2017).

[7] Hesketh, P. J., Zemel, J. N., and Gebhart, B., "Organ pipe radiant modes of periodic micromachined silicon surfaces," *Nature* **324**(6097), 549–551 (1986).

[8] Greffet, J.-J., Carminati, R., Joulain, K., Mulet, J.-P., Mainguy, S., and Chen, Y., "Coherent emission of light by thermal sources," *Nature* **416**, 61–64 (Mar. 2002).

[9] Dahan, N., Niv, A., Biener, G., Gorodetski, Y., Kleiner, V., and Hasman, E., "Enhanced coherency of thermal emission: beyond the limitation imposed by delocalized surface waves," *Phys. Rev. B* **76**, 045427 (Jul 2007).

[10] Puscasu, I. and Schaich, W. L., "Narrow-band, tunable infrared emission from arrays of microstrip patches," *Applied Physics Letters* **92**(23), 233102 (2008).

[11] Liu, X., Tyler, T., Starr, T., Starr, A. F., Jokerst, N. M., and Padilla, W. J., "Taming the blackbody with infrared metamaterials as selective thermal emitters," *Phys. Rev. Lett.* **107**, 045901 (Jul 2011).

[12] Makhsiyan, M., Bouchon, P., Jaeck, J., Pelouard, J.-L., and Hadar, R., "Shaping the spatial and spectral emissivity at the diffraction limit," *Applied Physics Letters* **107**(25) (2015).

[13] Ilic, O., Bermel, P., Chen, G., Joannopoulos, J. D., Celanovic, I., and Soljai, M., "Tailoring high-temperature radiation and the resurrection of the incandescent source," *Nat Nano* **11**, 320–324 (Apr. 2016).

[14] Vassant, S., Archambault, A., Marquier, F., Pardo, F., Gennser, U., Cavanna, A., Pelouard, J. L., and Greffet, J. J., "Epsilon-near-zero mode for active optoelectronic devices," *Phys. Rev. Lett.* **109**, 237401 (Dec 2012).

[15] Vassant, S., Doyen, I. M., Marquier, F., Pardo, F., Gennser, U., Cavanna, A., Pelouard, J. L., and Greffet, J. J., "Electrical modulation of emissivity," *Applied Physics Letters* **102**(8), 081125 (2013).

[16] Inoue, T., Zoysa, M. D., Asano, T., and Noda, S., "Realization of dynamic thermal emission control," *Nat Mater* **13**, 928–931 (Oct. 2014).

[17] Hildenbrand, J., Korvink, J., Wollenstein, J., Peter, C., Kurzinger, A., Naumann, F., Ebert, M., and Lamprecht, F., "Micromachined mid-infrared emitter for fast transient temperature operation for optical gas sensing systems," *IEEE Sensors Journal* **10**, 353–362 (Feb 2010).

[18] Sakat, E., Wojszvzyk, L., Hugonin, J.-P., Besbes, M., Sauvan, C., and Greffet, J.-J., "Enhancing thermal radiation with nanoantennas to create infrared sources with high modulation rates," *Optica* **5**, 175–179 (Feb 2018).

[19] Greffet, J.-J., Bouchon, P., Brucoli, G., Sakat, E., and Marquier, F., "Generalized kirchhoff law," *ArXiv 1601.00312* (Jan. 2016).

[20] Tretyakov, S., "Maximizing absorption and scattering by dipole particles," *Plasmonics* **9**(4), 935944 (2014).

[21] Fleury, R., Soric, J., and Alù, A., "Physical bounds on absorption and scattering for cloaked sensors," *Phys. Rev. B* **89**, 045122 (Jan 2014).

[22] Miller, O. D., Hsu, C. W., Reid, M. T. H., Qiu, W., DeLacy, B. G., Joannopoulos, J. D., Soljačić, M., and Johnson, S. G., "Fundamental limits to extinction by metallic nanoparticles," *Phys. Rev. Lett.* **112**, 123903 (Mar 2014).

[23] Grigoriev, V., Bonod, N., Wenger, J., and Stout, B., "Optimizing nanoparticle fesigns for ideal absorption of light," *ACS Photonics* **2**(2), 263–270 (2015).

[24] Colom, R., Devilez, A., Bonod, N., and Stout, B., "Optimal interactions of light with magnetic and electric resonant particles," *Phys. Rev. B* **93**, 045427 (Jan 2016).

[25] Miller, O. D., Polimeridis, A. G., Reid, M. T. H., Hsu, C. W., DeLacy, B. G., Joannopoulos, J. D., Soljačić, M., and Johnson, S. G., "Fundamental limits to optical response in absorptive systems," *Opt. Express* **24**, 3329–3364 (Feb 2016).

[26] Ivanenko, Y., Gustafsson, M., and Nordebo, S., "Optical theorems and physical bounds on absorption in lossy media," *Opt. Express* **27**, 34323–34342 (Nov 2019).

[27] Castanie, E., Vincent, R., Pierrat, R., and Carminati, R., "Absorption by an optical dipole antenna in a structured environment," *International Journal of Optics* , 452047 (2012).

[28] Sentenac, A., Chaumet, P. C., and Leuchs, G., "Total absorption of light by a nanoparticle: an electromagnetic sink in the optical regime," *Opt. Lett.* **38**, 818–820 (Mar 2013).

[29] Jackson, J. D., [*Classical Electrodynamics*], J. Wiley and Sons, New York (1974).

[30] Rytov, S. M., Kravtsov, Y. A., and Tatarskii, V. I., [*Principles of statistical radiophysics 2. Correlation theory of random processes.*] (1988).

[31] Purcell, E. M., "Spontaneous emission probabilities at radio frequencies," *Phys. Rev.* **69**, 681 (1946).

[32] Goy, P., Raimond, J.-M., Gross, M., and Haroche, S., "Observation of cavity-enhanced single-atom spontaneous emission," *Phys. Rev. Lett.* **50**(24), 1903–1906 (1983).

[33] Sauvan, C., Hugonin, J.-P., Maksymov, I. S., and Lalanne, P., "Theory of the spontaneous optical emission of nanosize photonic and plasmon resonators," *Phys. Rev. Lett.* **110**, 237401 (2013).

[34] Seok, T. J., Jamshidi, A., Kim, M., Dhuey, S., Lakhani, A., Choo, H., Schuck, P. J., Cabrini, S., Schwartzberg, A. M., Bokor, J., Yablonovitch, E., and Wu, M. C., "Radiation engineering of optical antennas for maximum field enhancement," *Nano Letters* **11**(7), 2606–2610 (2011). PMID: 21648393.

[35] Metzger, B., Hentschel, M., Schumacher, T., Lippitz, M., Ye, X., Murray, C. B., Knabe, B., Buse, K., and Giessen, H., "Doubling the efficiency of third harmonic generation by positioning ito nanocrystals into the hot-spot of plasmonic gap-antennas," *Nano Letters* **14**(5), 2867–2872 (2014). PMID: 24730433.

[36] Balanis, C. A., [*Antenna theory: Analysis and design*], J. Wiley and Sons, New York, second ed. (1997).

[37] Andersen, J. B., "Absorption efficiency of receiving antennas," *IEEE Transactions on Antennas and Propagation* **53**(9), 2843 – 289 (2005).

[38] Ra'di, Y. and Tretyakov, S. A., "Balanced and optimal bianisotropic particles: maximizing power extracted from electromagnetic fields," *New Journal of Physics* **15**(5), 053008 (2013).

[39] Greffet, J.-J., Laroche, M., and Marquier, F., "Impedance of a nanoantenna and a single quantum emitter," *Phys. Rev. Lett.* **105**, 117701 (Sep 2010).

[40] Sakat, E., Wojszvzyk, L., Greffet, J.-J., Hugonin, J.-P., and Sauvan, C., "Enhancing light absorption in a nanovolume with a nanoantenna: Theory and figure of merit," *ACS Photonics* **7**(6), 1523–1528 (2020).

[41] Bigourdan, F., Hugonin, J.-P., and Lalanne, P., "Aperiodic-fourier modal method for analysis of body-of-revolution photonic structures," *J. Opt. Soc. Am. A* **31**, 1303–1311 (Jun 2014).

[42] Lalanne, P., Yan, W., Vynck, K., Sauvan, C., and Hugonin, J.-P., "Light interaction with photonic and plasmonic resonances," *Laser Photonics Rev.* **12**, 1700113 (2018).

[43] Stout, B., Auger, J.-C., and Lafait, J., "A transfer matrix approach to local field calculations in multiple-scattering problems," *Journal of Modern Optics* **49**(13), 2129–2152 (2002).

[44] Stout, B., Devilez, A., Rolly, B., and Bonod, N., "Multipole methods for nanoantennas design: applications to yagi-uda configurations," *J. Opt. Soc. Am. B* **28**, 1213–1223 (May 2011).

[45] Mendelsberg, R. J., Garcia, G., and Milliron, D. J., "Extracting reliable electronic properties from transmission spectra of indium tin oxide thin films and nanocrystal films by careful application of the drude theory," *Journal of Applied Physics* **111**(6), 063515 (2012).

[46] Mendelsberg, R. J., Garcia, G., Li, H., Manna, L., and Milliron, D. J., "Understanding the plasmon resonance in ensembles of degenerately doped semiconductor nanocrystals," *The Journal of Physical Chemistry C* **116**(22), 12226–12231 (2012).